On the Effect of Sweat on Sheet Resistance of Knitted Conductive Yarns in Wearable Antenna Design

Md Abu Saleh Tajin, Ariana S. Levitt, Yuqiao Liu, *Student Member, IEEE*, Chelsea E. Amanatides, Caroline L. Schauer, Genevieve Dion, and Kapil R. Dandekar, *Senior Member, IEEE*

***Abstract*—Researchers are looking for new methods to integrate sensing capabilities into textiles while maintaining the durability, flexibility, and comfort of the garment. One method for imparting sensing capabilities into garments is through coupling conductive yarns with the radio frequency identification (RFID) technology. These smart devices have exhibited promising results for short-term use. However, long-term studies of their performance are still needed to evaluate their performance over a longer period. Like all garments, wearable sensors are susceptible to environmental factors during use. These factors can lead to dielectric coupling and corrosion of conductive yarns, which has the potential to degrade the performance of the device. This letter analyzes the effect of sweat and moisture on silver-coated nylon yarn by extracting the sheet resistance at 913 MHz from transmission line measurements. HFSS simulation shows the level of perturbation in antenna performance as sheet resistance increased with each cycle of sweat-immersion, washing, and drying.**

***Index Terms*—Digital fabrication, radio frequency identification (RFID), sheet resistance, silver-coated nylon, textile antennas.**

I. Introduction

SEAMLESS integration of electronic devices into textile structures has been a major focus of the smart textile community since its beginning; how to turn fabrics into interactive interfaces where the textiles themselves are the devices. Radio frequency identification (RFID) technology has been used for decades in a variety of applications for identification and tracking purposes [1]–[3], and the general procedure for designing and optimizing traditional tag antennas is well established. The combination of modeling and experimental studies has expanded the breadth of applications for RFID systems to emerging technologies such as wearable health monitoring systems. These systems are used to track physiological measures, such as the heart rate of a user [4]–[6].

For wearable applications, researchers have investigated the integration of antennas into textile structures using conductive fibers and yarns, which provide a flexible pathway for conducting electrical current [7], [8]. Silver-coated nylon yarns, one of the most available conductive yarns used in wearable smart garments, exhibit good electronic properties, but are easily damaged and are susceptible to environmental factors like moisture and sweat [9]. Currently, the design process for textile antennas using these yarn materials remains to a large extent a long series of prototyping experiments, where changes in the design can only be fully understood after a sample is fabricated and evaluated. To minimize the consumption of excessive materials and time, it is necessary to develop a parametric modeling software that can predict the performance of textile antennas based on mechanical deformation and environmental effects (e.g., moisture, sweat, oxidation, etc.).

This letter presents a new approach for optimizing knit antenna design for dynamic environments by extracting sheet resistance at 913 MHz. Sheet resistance can be used to accurately predict the antenna performance and reduce the lengthy prototyping period. Instead of using textile antennas with RFID transponders, fabric-based transmission lines are used to study the effect of sweat. The advantages are twofold. First, sweat and moisture can be directly introduced to the transmission line without worrying about the RFID chip getting soaked. Second, sheet resistance can be calculated from the *S*-parameter measurements of the transmission line. Measured sheet resistances are used to simulate antenna performance in a dynamic environment.

II. Related Work

Chui *et al.* studied the performance of silver-coated nylon yarns in dynamic environments and found that the dc resistance of the yarn changed with exposure to temperature and friction [9]. However, high-frequency resistance needs to be studied. Fu *et al.* [10] studied the washing durability of textile ultrahigh frequency RFID tags based on dipole antennas fabricated from silver fabric and found that the read-range decreased after consecutive washing cycles. The antenna-IC joint was covered with textile glues that potentially changes the tag performance. He *et al.* [11] showed that the read-range of 3-D printed graphene

Manuscript received January 20, 2020; accepted January 29, 2020. Date of publication February 3, 2020; date of current version April 17, 2020. This work was supported in part by the National Science Foundation under Grant CNS-1816387, in part by the National Institutes of Health under Grant R01-EB029364, and in part by the National Science Foundation Graduate Research Fellowship under Grant DGE-1646737 and Grant DGE-10028090/DGE-1104459. The work of Ariana S. Levitt was supported by the National Science Foundation Graduate Research Fellowship under Grant DGE-1646737. *(Md Abu Saleh Tajin and Ariana Levitt contributed equally to this work.) (Corresponding author: Md Abu Saleh Tajin.)*

Md Abu Saleh Tajin, Yuqiao Liu, and Kapil R. Dandekar are with the Department of Electrical and Computer Engineering, Drexel University, Philadelphia, PA 19104 USA (e-mail: mt3223@drexel.edu; yl636@drexel.edu; dandekar@drexel.edu).

Ariana S. Levitt, Chelsea E. Amanatides, and Caroline L. Schauer are with the Materials Science and Engineering Department, Drexel University, Philadelphia, PA 19104 USA (e-mail: asl95@drexel.edu; cek56@drexel.edu; cls52@drexel.edu).

Genevieve Dion is with the Design Department, Drexel University, Philadelphia, PA 19104 USA (e-mail: gd63@drexel.edu).

Digital Object Identifier 10.1109/LAWP.2020.2971189

Fig. 1. Bellyband antenna.

antennas is reduced by the introduction of moisture. However, the read-range returns to normal after drying. Scarpello *et al.* [12] and Toivonen *et al.* [13] found that radiation efficiencies of fabric-based antennas drop with washing cycles.

III. Antenna Materials, Design, and Simulation

When incorporating antennas into garment devices, a number of requirements must be met in addition to the technical specifications of an antenna, such as read-range and sheet impedance [14]. Ideally, wearable antennas should be unobtrusive, comfortable, lightweight, robust, and low-maintenance, meaning that they can withstand similar treatment to that of a conventional garment without loss of functionality [15]. Textile devices have the added demands of maintaining the same performance level of conventional devices while being subjected to a variety of environments such as exposure to sweat and moisture.

Taking these requirements into consideration, and leveraging RFID technology in textiles, a knitted Bellyband antenna was developed, detailed in [16] and [17] and shown in Fig. 1, a wireless and battery-free smart garment for pregnant women designed to monitor uterine contractions. To the best of authors' knowledge, we are among the first to investigate the use of passive RFID systems in wearable garments. The Bellyband design in [16] and [17] uses both conductive silver yarns and nonconductive yarns and a small RFID tag is inserted into the band during knitting. The Bellyband is designed, programmed, and manufactured using computer-aided weft knitting techniques.

While the Bellyband antenna performed well in free space, it was not designed to accommodate for environmental changes and on-body effects. In order to better design the antenna for these situations, it is necessary to understand the effect of the real and imaginary parts of the sheet impedance on the *S*-parameters. To do this, a two-port microstrip structure is simulated. A complex value of sheet impedance (Z_s) is assigned to a 2-D structure in order to model the top part of a microstrip structure and the ground layer was modeled with copper. The real part (R_s) of the sheet impedance is related to the resistance of conductor material, while the imaginary part (X_s) is related to the electric field distribution in the substrate. The simulation results shown in Fig. 2 can be summarized as follows.

1) If R_s is fixed, $|S_{21}|$ does not change much (approximately 0.1 dB) while sweeping the X_s parameter.
2) If X_s is fixed, increasing R_s causes dramatic increase (around 1.0 dB) in $|S_{21}|$.

From a simulation point of view, to better predict the performance of a fabric-based antenna, a proper knowledge of the real part of the sheet impedance is more crucial than its imaginary counterpart. As a result, the aim is to extract the sheet resistance and investigate its nature as the fabric goes through cycles of sweat, washing, and drying.

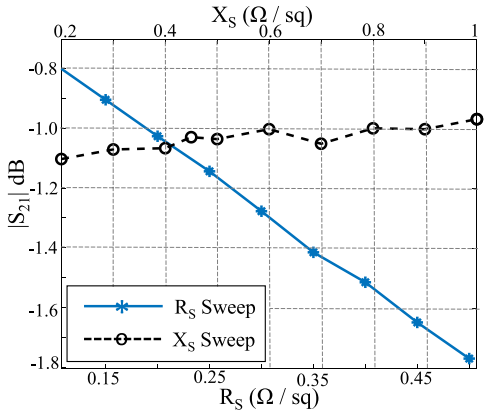

Fig. 2. $|S_{21}|$ versus R_S and X_S plot. $|S_{21}|$ is highly sensitive to any change in R_S. In contrast, X_S does not change $|S_{21}|$ that much.

IV. Measurement Setup

To inform and validate this model, knitted transmission lines are fabricated to the dimensions of the simulated antennas (8 cm $\times$ 2 cm). The same conductive and nonconductive yarns, stitch values, and knit structures as used to knit the Bellyband in [16] and [17] are used to knit these simplified antennas. Samples are programmed using Shima Seikis SDS-ONE APEX3 design system and knitted on an SSG-122SV Shima Seiki knitting machine. After knitting, the samples are attached to an FR4-based single-sided printed circuit board (PCB). To ensure consistent measurements, three transmission lines are fabricated. A similar structure is also constructed with copper on both sides of the substrate. To understand the effect of everyday use on antenna performance, the knitted transmission lines are subjected to artificial sweat (AS) for a period of seven days to determine the effect of sweat and moisture on antenna performance, specifically on their sheet resistance. The AS was prepared according to EN 1811 by combining NaCl (5.0 g/L), lactic acid (1.0 g/L), and urea (1.0 g/L). The pH was adjusted to 6.5 using NaOH. The knitted samples are submerged in AS for seven days and measurements are taken every 24 h. Samples are rinsed in deionized water and dried in an oven for 20 min at 80 °C before taking measurements. *S*-parameter measurements are taken using an N5230 A agilent vector network analyzer in the frequency range of 0.5–3 GHz. Both ends of the PCB are connected to the network analyzer using two 50 SMA feeds.

V. Parameter Extraction

A. "R" Parameter

A transmission line can be described by distributed R (Ω/m), L (nH/m), C (pF/m), and G (S/m) parameters (see Fig. 3). Although the S-parameters of a transmission line are convenient to measure with network analyzers, resistance, inductance, capacitance and conductance (RLCG) parameters cannot be extracted directly from scattering parameters. First, ABCD parameters

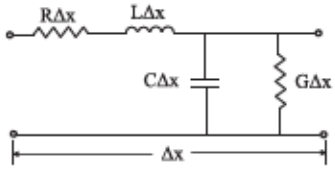

Fig. 3. Distributed RLCG parameter model of a transmission line.

need to be calculated from S-parameters, and then we can calculate RLCG parameters. We are studying the corrosion of silver-coated nylon yarns by evaluating its sheet resistance under the exposure to sweat. In theory, the mere presence (corrosion not considered) of sweat in a conducive fabric should only affect the dielectric property part (G). The resistive part (R) would remain unaffected as it is coming from conductive losses. We use the "R" parameter ($R_{\rm m}$) to extract sheet resistance of the knitted conductive fabric [18] as

$$R_{\rm m} = Re(\gamma Z_{\rm c}) \tag{1}$$

where $R_{\rm m}(\Omega/m)$ is the series resistance per unit length, γ is the complex propagation constant, and Z_c is the characteristic impedance of the transmission line. γ and Z_c are related to the RLCG parameters by the following equations:

$$\gamma = \sqrt{(R + j\omega L)(G + j\omega C)} \tag{2a}$$

$$Z_{\rm c} = \sqrt{\frac{(R + j\omega L)}{(G + j\omega C)}}. \tag{2b}$$

The direct extraction of $R_{\rm m}$ using (1) leads to an ill-posed mathematical problem [19], giving rise to unexpectedly sharp and large peaks, and even negative values. A previous study [19] has shown that the propagation constant is less affected by the hyperbolic behavior. The propagation constant (γ) was accepted, and the characteristic impedance (Z_c) was discarded. Z_c was later optimized, based on S-parameters, using the interior-point method.

B. Sheet Resistance

The sheet resistance of the conductive fabric needs to be extracted at the frequency of interest (913 MHz). At 913 MHz, skin depth of copper ($\delta_{\rm cu}$) can be calculated

$$\delta_{\rm cu} = \sqrt{\frac{\rho_{\rm cu}}{\pi f \mu_{\rm cu}}} = 2.16\,\mu{\rm m}$$

where $\rho_{\rm cu}$ ($1.68 \times 10^{-8}\,\Omega - {\rm m}$) is the resistivity of copper, $f =$ 913 MHz, $\mu_{\rm cu}(\approx 4\pi \times 10^{-7}{\rm H/m})$ is the magnetic permeability of copper. As a result, the sheet resistance ($R_{\rm sg}$) of the ground layer at 913 MHz is

$$R_{\rm sg} = \frac{\rho_{\rm cu}}{\delta_{\rm cu}} = 7.77\ {\rm m}\Omega/{\rm sq}.$$

The thickness (35.6 mm) of the copper ground layer is many times larger than the skin depth (2.16 μm) at 913 MHz. Simulation results shows (see Fig. 4) that current flows in the ground layer with an effective width, approximately three times the width of the top layer. The resistance of the ground copper

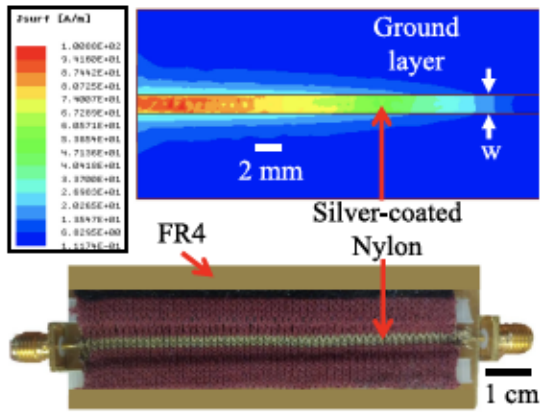

Fig. 4. (Top) Simulated surface current density at the top (conductive fabric) and bottom (copper) layer, (bottom) conductive fabric-based microstrip transmission line structure.

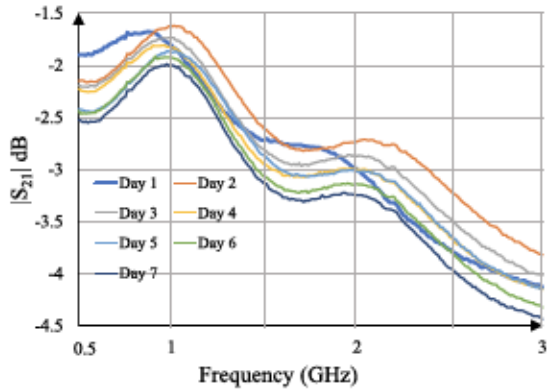

Fig. 5. S_{21} of the fabric-based transmission line (sample-1) as a function of exposure to AS.

structure (80 mm $\times$ 6 mm $\times$ 2.16 μm), $R_{\rm gnd} = 0.1\ \Omega$. From RLCG extraction, the per unit length resistance (R) of the unaltered (day-1, no sweat added) transmission line was found 173.4 Ω/m.

Total conductor losses of the structure can be attributed to the resistive losses occurring in the top layer (made of lossy conductive fabric) and the ground layer (made of copper) [20], and the radiation resistance. Total resistance of the microstrip transmission line (80 mm in length) at 913 MHz is the summation of the radiation and loss resistances [21] calculated as

$$R_{\rm total} = R_{\rm fab} + R_{\rm gnd} + R_{\rm rad} = 14.64\ \Omega. \tag{3}$$

The sheet resistance of the silver-coated nylon is

$$R_{\rm sr} = R_{\rm fab}\left(\frac{w}{L}\right) \tag{4}$$

where w and L are the width and length of the top layer of the transmission line.

VI. Results and Discussion

Measured $|S_{21}|$ (see Fig. 5) shows that with the introduction of sweat (days 2–6), losses inside the fabric-based two-port transmission line increase. On the other hand, the standard

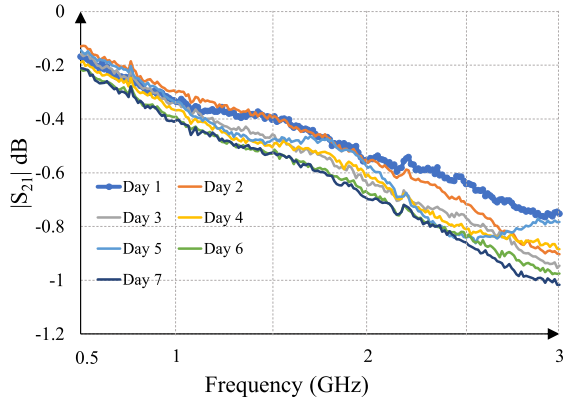

Fig. 6. S_{21} of the standard copper-based transmission line as a function of exposure to AS.

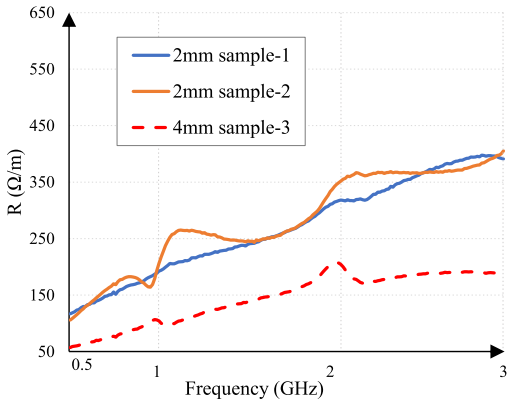

Fig. 7. Extracted per unit length resistance (R-parameter) of two fabric-based transmission line samples on day-1.

double-sided copper-based transmission line does not demonstrate a similar pattern of degradation (see Fig. 6). On day-2, the transmission line undergoes the first cycle of sweat, washing, and the $|S_{21}|$ of that day has a different peak location (at around 1 GHz). With each cycle, the loss increases and the peak does not return to its previous position (day-1). It means that the characteristic impedance of the transmission line was permanently changed after the first washing cycle. Extracted R-parameter of the unaltered fabric transmission line is presented in Fig. 7. The sheet resistance ($R_{\rm sr}$) of the silver-coated nylon can be calculated using (4). On day-1, $R_{\rm sr}$ was 0.34 Ω/sq. HFSS simulation shows that the similar value of $|S_{21}|$ at 913 MHz is found for $R_{\rm sr} = 0.4\ \Omega$/sq, which is very close to the measured value. This mismatch can be attributed to the imperfect SMA-fabric interfaces on both terminals of the transmission line. Moreover, in HFSS, the top fabric layer was modeled as a perfect rectangle, whereas in reality, very small wedges exist as a result of knitting.

With the introduction of sweat, the sheet resistance of the fabric shows an increasing trend. This is likely due to the silver coating delaminating from the surface of the nylon fibers upon exposure to sweat, washing, and drying. Consequently, the resistive loss in the antenna increases. This increase in the internal loss mainly affects the fabric antenna in two ways. First, the radiation efficiency declines with increased loss. HFSS

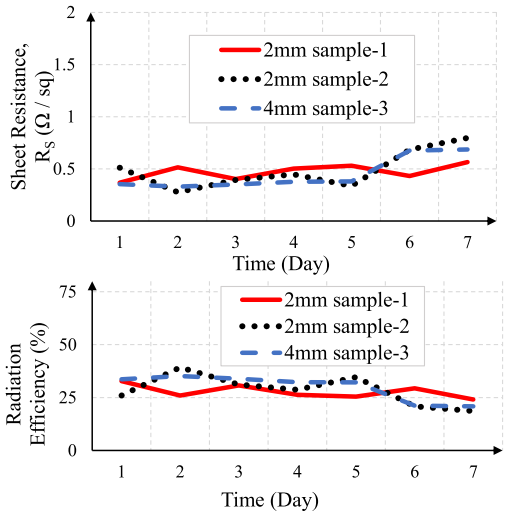

Fig. 8. Extracted sheet resistance and simulated radiation efficiency of the fabric antennas at 913 MHz versus time.

simulation of the fabric-based bellyband antenna shows that after undergoing cycles of sweat-immersion, washing, and drying for six days, the radiation efficiency of the antenna decayed from 32.7% to 24% (see Fig. 8, sample-1). At 913 MHz, this degradation in radiation efficiency represents a reduction in read-range by 0.17 m (10% of initial value 1.6 m [22]). On the other hand, the impedance match between the RFID chip and the antenna might be affected due to a change in antenna input impedance. However, HFSS simulation shows that over seven days of experimentation, the input impedance of the antenna changed from $(12.6 + j176.02)\ \Omega$ to $(17.1 + j175.95)\ \Omega$. Compared to the reduction in radiation efficiency, this small variation in impedance mismatch does not result in any significant change in read-range.

VII. Conclusion

This letter presents a new method to extract the fabric-based antenna design parameter (sheet resistance) in a dynamic environment. The effects of sweat on sheet resistance of silver-coated nylon (at 913 MHz) and radiation efficiency of the antenna are studied. This letter shows that silver-coated nylon is vulnerable to sweat and washing cycles. The extracted surface resistance values would facilitate the precalculation of antenna performance in a dynamic environment. This, in turn, will facilitate the machine learning technique that is being used to identify the uterine activity and respiration rate. Ultimately, a parametric software will create the opportunity for minimization of the prototyping stages of design and ensure a faster transition from research to commercialization.

Acknowledgment

The authors would like to thank R. Lehrich and C. Kara for their assistance with antenna fabrication. The authors made use of Drexels Core Research Facilities. Any opinion, findings, and conclusion or recommendations expressed in this work are those of the author(s) and do not necessarily reflect the views of the National Science Foundation or the National Institutes of Health.

REFERENCES

[1] V. Chawla and D. S. Ha, "An overview of passive RFID," *IEEE Commun. Mag.*, vol. 45, no. 9, pp. 11–17, Sep. 2007.

[2] A. Moraru, E. Helerea, C. Ursachi, and M. D. Clin, "RFID system with passive RFID tags for textiles," in *Proc. 10th Int. Symp. Adv. Topics Elect. Eng.*, 2017, pp. 410–415.

[3] K. S. Rao, P. V. Nikitin, and S. F. Lam, "Antenna design for UHF RFID tags: A review and a practical application," *IEEE Trans. Antennas Propag.*, vol. 53, no. 12, pp. 3870–3876, Dec. 2015.

[4] G. Marrocco, "RFID antennas for the UHF remote monitoring of human subjects," *IEEE Trans. Antennas Propag.*, vol. 55, no. 6, pp. 1862–1870, Jun. 2007.

[5] C. Occhiuzzi, S. Cippitelli, and G. Marrocco, "Modeling, design and experimentation of wearable RFID sensor tag," *IEEE Trans. Antennas Propag.*, vol. 58, no. 8, pp. 2490–2498, Aug. 2010.

[6] S. Amendola, R. Lodato, S. Manzari, C. Occhiuzzi, and G. Marrocco, "RFID technology for IoT-based personal healthcare in smart spaces," *IEEE Internet Things J.*, vol. 1, no. 2, pp. 144–152, Apr. 2014.

[7] X. Qing, C. K. Goh, and Z. N. Chen, "Impedance characterization of RFID tag antennas and application in tag co-design," *IEEE Trans. Microw. Theory Techn.*, vol. 57, no. 5, pp. 1268–1274, May 2009.

[8] E. Moradi, T. Björninen, L. Ukkonen, and Y. Rahmat-Samii, "Effects of sewing pattern on the performance of embroidered dipole-type RFID tag antennas," *IEEE Antennas Wireless Propag. Lett.*, vol. 11, pp. 1482–1485, 2012.

[9] Y. T. Chui, C. X. Yang, J. H. Tong, Y. F. Zhao, C. P. Ho, and L. L. Li, "A systematic method for stability assessment of Ag-coated nylon yarn," *Textile Res. J.*, vol. 86, no. 8, pp. 787–802, 2015.

[10] Y. Y. Fu *et al.*, "Experimental study on the washing durability of electro-textile UHF RFID tags," *IEEE Antennas Wireless Propag. Lett.*, vol. 14, pp. 466–469, 2015.

[11] H. He, M. Akbari, L. Sydänheimo, L. Ukkonen, and J. Virkki, "3D-printed graphene antennas and interconnections for textile RFID tags: Fabrication and reliability towards humidity," *Int. J. Antennas Propag.*, vol. 2017, pp. 1–5, 2017.

[12] M. L. Scarpello, I. Kazani, C. Hertleer, H. Rogier, and D. Vande Ginste, "Stability and efficiency of screen-printed wearable and washable antennas," *IEEE Antennas Wireless Propag. Lett.*, vol. 11, pp. 838–841, 2012.

[13] M. Toivonen, T. Bjorninen, L. Sydanheimo, L. Ukkonen, and Y. Rahmat-Samii, "Impact of moisture and washing on the performance of embroidered UHF RFID tags," *IEEE Antennas Wireless Propag. Lett.*, vol. 12, pp. 1590–1593, 2013.

[14] T. Bashir, "Conjugated polymer-based conductive fibers for smart textile applications," Ph.D. dissertation, Chalmers Univ. Tech., 2013.

[15] D. Cottet, J. Grzyb, T. Kirstein, and G. Tröster, "Electrical characterization of textile transmission lines," *IEEE Trans. Adv. Packag.*, vol. 26, no. 2, pp. 182–190, May 2003.

[16] D. Patron *et al.*, "On the use of knitted antennas and inductively coupled RFID tags for wearable applications," *IEEE Trans. Biomed. Circuits Syst.*, vol. 10, no. 6, pp. 1047–1057, Dec. 2016.

[17] Y. Liu, A. Levitt, C. Kara, C. Sahin, G. Dion, and K. R. Dandekar, "An improved design of wearable strain sensor based on knitted RFID technology," in *Proc. IEEE Conf. Antenna Meas. Appl.*, 2017, pp. 1–4.

[18] I. Kiirgad, N. Dagli, G. L. Matthaei, and S. I. Long, "Experimental analysis of transmission line parameters in high-speed GaAs digital circuit interconnects," *IEEE Trans. Microw. Theory Techn.*, vol. 39, no. 8, pp. 1361–1367, Aug. 1991.

[19] R. Papazyan, P. Pettersson, H. Edin, R. Eriksson, and U. Gäfvert, "Extraction of high frequency power cable characteristics from S-parameter measurements," *IEEE Trans. Dielectr. Elect. Insul.*, vol. 11, no. 3, pp. 461–470, Jun. 2004.

[20] R. Faraji-Dana and Y. L. Chow, "The current distribution and AC resistance of a microstrip structure," *IEEE Trans. Microw. Theory Techn.*, vol. 38, no. 9, pp. 1268–1277, Sep. 1990.

[21] C. A. Balanis, *Antenna Theory: Analysis and Design*. Hoboken, NJ, USA: Wiley, 2005, p. 81.

[22] M. A. S. Tajin, O. Bshara, Y. Liu, A. Levitt, G. Dion, and K. R. Dandekar, "Efficiency measurement of the flexible on-body antenna at varying levels of stretch in a reverberation chamber," *Microw., Antennas Propag.*, vol. 14, no. 3, pp. 154–158, Jul. 2019.